Hindawi
Journal of Engineering
Volume 2022, Article ID 9558553, 13 pages
https://doi.org/10.1155/2022/9558553

Research Article

Simulation of Separation of Salt Solution from Crude Oil in a Hydrocyclone

Mansour Mohammadi,[1] Amir Sarafi,[1] Ataallah Kamyabi,[1] Ataallah Soltani Goharrizi,[1] and Bahador Abolpour[2]

[1]*Department of Chemical Engineering, Shahid Bahonar University of Kerman, Kerman, Iran*
[2]*Department of Chemical Engineering, Sirjan University of Technology, Sirjan, Iran*

Correspondence should be addressed to Bahador Abolpour; bahadorabolpor1364@yahoo.com

Received 3 March 2022; Revised 16 May 2022; Accepted 30 May 2022; Published 6 July 2022

Academic Editor: Chong Leong Gan

In this study, separating water from oil is studied numerically. In this simulation, the Reynolds Stress Model and the mixture multiphase model are used for coupling the velocity and pressure equations using the SIMPLE algorithm. The simulated geometry is taken from an experimental setup. It results that, in the case of the crude oil as the discrete phase, by increasing the diameter of the discrete phase (crude oil) droplets, the separation efficiency increases. If the diameter of the oil droplets is greater than 100 microns, the percentage of oil output from the spillway reaches 99.5%. In the case of the water phase as the discrete phase, if the water droplets size is considered equal to 200 microns, the water separation efficiency in the spillway reaches 69%.

1. Introduction

Today's refinery operations are very complex, and for a person unfamiliar with the industry, it seems impossible to reduce this complexity and present the operation as a coordinated set of simple processes. The refinery aims to convert more crude oil into transportation fuels with practical economic aspects. Although refineries produce such useable products, a large proportion of their useable products are transport fuels such as gasoline, diesel, turbine (jet) fuels, and light heating oils. The quality of crude oil used for processing in refineries is not quantified. They determine what is in it. Crude oil received from wells is accompanied by some water. In the water that comes out of the wells with oil, some salts are dissolved, such as magnesium and calcium salts. The amount of this solution is alternating. For example, in Middle Eastern oils, it is about 12 grams per ton, and in Egypt oils, it is about 3 kg per ton. If the amount of salt in crude oil exceeds 38 grams per cubic meter, it should be desalinated. Another important parameter is the percentage of salt and water sediments associated with oil, which is determined by the BS&W parameter. Therefore, many refineries desalinated for less than this amount [1, 2]. Excessive saltwater in oil causes four major problems and frequent financial losses because of the following:

(i) Water becomes highly corrosive due to the presence of soluble salts and causes perforation and permanent destruction of expensive devices and equipment such as pipes, valves, tanks, and oil tankers.

(ii) The presence of solute deposits on the inner surface of the devices and equipment of refineries causes clogging and increases pressure drop, and disrupts their performance. Blocks the pipes of oil heaters, causing heat and pressure to rise and rupture, leading to catastrophic explosions and fires.

(iii) It pierces the inner parts of the distillation towers, causing them to shut down and require repair, which yields heavy costs. Therefore, water should be prevented from entering the refinery equipment as much as possible.

(iv) If water is not separated from the oil, in addition to the mentioned losses, it will occupy a part of the volume of oil reservoirs and pipes, and as a result, the volume of sent oil will be reduced, and water transportation that has no value will have costs equal to oil transportation costs.

Crude oil contains different amounts of inorganic salts (NaCl, $CaCl_2$, $MgCl_2$, etc.). The presence of these salts during the processing of crude oil causes some problems, such as corrosion, connection and deposition of equipment, and poisoning of catalysts in the processing units. The desalination process is done by washing the crude oil with clean water and then removing the water to separate the salt from the crude oil [3]. The process of desalination and effective separation of the dispersed phase of brine from the continuous oil phase is a desirable process that has a variety of methods. For example, gravity, suspension, thermal performance, and electrostatic coagulation are methods used to separate brine from crude oil. Each of these methods has advantages and disadvantages. One of the most common methods in the desalination process is the electric method, but the operational complexity and high operating costs are many disadvantages of electrical desalination. Many research institutes have developed desalination methods and have recently made great strides, including the centrifuge method, the filtration method, the magnetic control method, the microwave irradiation method, and so on. However, these methods are less used in industrial production due to the complexity of equipment and low reliability [4]. The principle of operation of hydrocyclone is similar to that of a centrifuge, except that the body of a hydrocyclone is fixed and the fluid inside it rotates. A hydrocyclone includes an inlet, cylindrical, reduction, conical, tailpipe, bottom pipe, and overflow sections. The flow is injected tangentially into the cylindrical section of the hydrocyclone. As a result of the rotation of the fluid inside the body, two internal and external vortices are formed.

Hsieh and Rajamani [5] 1991 developed a mathematical model of a hydrocyclone based on fluid flow physics. Their model equations were solved using a computer code that considered the dimensions of the hydrocyclone and the properties of the feed slurry as input. The Navier-Stokes governing equations for the hydrocyclone geometry were successfully solved. The output of their computer code was the fluid velocity profile and the separation efficiency curve. The predictions of their model were validated using the measured velocity profile inside a 75 mm hydrocyclone. Pure water and glycerol-water mixture were used as a working fluid to simulate the increment of the slurry viscosity in the presence of solid particles. In 2001, Gomez et al. [6] numerically modeled and experimentally experimented with the separation of an oil-water mixer in a 2-inch hydrocyclone. Their goal was to develop mechanical modeling for oil removal. The inputs required for their model included fluid properties, inlet droplet size distribution, and operating conditions. This model was able to predict the hydraulic flow field. Obtained data included flow rate and droplet size distribution at the inlet and downstream and oil concentration at the spillway and separation efficiency. They observed excellent agreement between model prediction and experimental data concerning separation efficiency and pressure drop. In 2002, Jiang et al. [7] investigated the effect of geometric and operational parameters on pressure drop and oil-water separation performance in hydrocyclones. Several hydrocyclone prototypes were investigated to obtain the effects of geometric parameters, including vortex cavity length and conical cross-section, and practical parameters. Their results showed that different geometric parameters of hydrocyclones should be selected in different conditions.

Reyes et al. [8] investigated in 2006 whether the computational fluid dynamics (CFD) method was able to simulate the liquid-liquid hydrocyclone behavior. The mixture of oil and water entering the hydrocyclone was divided into a high output (rich in oil) and a low output (rich in water) due to centrifugal and buoyancy forces. Separation efficiency was determined as the maximum amount of water discharged from the bottom of the minimum amount of oil at the bottom outlet or vice versa. Their experiments were performed in a transparent liquid-liquid separator, which allows the mixture to be visualized and the amount of oil to be measured. The experiments were performed on three variables mixing speed, water content at the inlet, and split ratio. Their results showed that the CFD tool was able to analyze the oil content obtained from the experiments for all conditions. This study confirmed the capacity of CFD instruments to analyze the multiphase flow of liquid-liquid separators. Bhaskar et al. [9] 2007 simulated a hydrocyclone with CFD and experimentally validated its results. In this research, an attempt was made to develop a method to simulate the performance of a hydrocyclone. They compared the experimental and simulated results using different turbulence models, namely the k-ε and Reynolds Stress Models (RSM). Among these modeling methods, the prediction using the RSM was found to agree with the experimental results with an acceptable final error. In 2007, Husveg et al. [10] studied the performance of hydrocyclones during variable flow rates and found that hydrocyclones are one of the newest technologies for treating offshore water. In the acceleration field inside the hydrocyclone, the oil was transferred to the center of the cyclone because the water was forced to stick to the wall. The separation depended on the structure of the double vortex flow within the hydrocyclone.

Bai and Wang [11] 2007 designed a desalination process of crude oil based on hydrocyclone technology. In this hydrocyclone, the salt concentration was reduced from 8 mg/l to 3 mg/l, and the dehydration efficiency was from 86 to 99%, with a feed flow rate from 27 to 30 m^3/hr. In 2010, Shi et al. [12] studied the liquid-liquid hydrocyclone cylinders and investigated the effect of design parameters, such as different diameters, different shapes, and the size of the vortex diameter at the top of the hydrocyclone, on the separation efficiency through experimental and simulation methods. The results showed that the diameter and angle of the vortex affect the rotational flow and the separation efficiency. Finally, they concluded that the size of oil droplets had a significant effect on separation. Increasing the average

droplet diameter or trying to prevent droplets from breaking into very small droplets was a practical way to improve the hydrocyclone separation efficiency. In 2011, Zang et al. [13] simulated the flow field inside a hydrocyclone with CFD according to the RNG k-ε model and the Eulerian method. The fluid flows in the cylindrical section and the conical section were very different. In the hydrocyclone separation process, the dispersed phase affects the continuous phase flow and complicates the turbulent flow field. There were still some shortcomings and errors in this model in multiphase hydrocyclone simulation. In 2012, Amini et al. [14] proposed a mathematical model to predict the efficiency of a low-cavity oil and water separation hydrocyclone. This separation efficiency was determined based on the droplet path of a continuous oil drop. The droplet path model is developed using the Lagrangian approach in which individual droplets are tracked in a continuous phase. This model uses a continuous phase rotation flow to track oil droplets, and the trial and error method is used to determine the size of the oil droplets that reach the reverse flow region. The inputs required for their model were the hydrocyclone geometry, fluid properties, inlet droplet size distribution, and operating conditions at the lower output. This model was able to predict the hydrodynamic flow field of the hydrocyclone, *i.e.,* the distribution of axial, tangential, and radial velocities of the continuous phase. Their results showed that the proposed model can well predict the ratio and separation efficiency of the hydrocyclone.

Narasimha et al. [15] 2012 predicted the particle separation in a rotating flow inside a 75 mm hydrocyclone. To simulate the performance of hydrocyclones, they used different turbulent multiphase CFD models. They found that in the two-phase simulations, the mean and turbulent stresses predicted by the Large Eddy Simulation model were in good agreement with the previously validated data. Hosseini et al. [16] 2015 investigated the parameters affecting the performance of oil remover hydrocyclones. In this study, the effects of inlet flow, inlet oil volume fraction, and diameter of oil droplets on separation efficiency and pressure drop ratio along the body of the hydrocyclone have been investigated. All simulations were performed using CFD techniques, in which the Eulerian multiphase model and the Reynolds turbulent stress model were used to predict the multiphase and turbulent flow parameters in hydrocyclone. Their simulation results showed a good agreement with the reported experimental data. Vakamalla and Mangaddodi [17] modeled turbulent flow inside an industrial hydrocyclone in 2017. Flow in industrial hydrocyclones is always turbulent. Therefore, choosing the right turbulent model for accurate prediction is one of the most important parts of the simulation. The goal of these two scientists was to find a suitable turbulent model for predicting rotational flow in industrial hydrocyclones. Two-phase and multiphase simulations in hydrocyclones of various industrial sizes are performed using fluidized-volume models modified with RSM, isolated vortex simulations, and LES. The simulated flow field velocities in the 75 and 250 mm hydrocyclones were measured using the laser Doppler measurement method. They concluded that the prediction of the turbulent RSM in larger hydrocyclones with low turbulence levels is reasonably good. But at the smaller sizes of hydrocyclones, the LES prediction is superior to other turbulent models. And the results they obtained suggested that the RSM could be used in larger hydrocyclones due to low turbulence levels. However, in smaller hydrocyclones, the LES turbulence model needs to be used for accurate prediction.

Liu et al. [18] 2018 presented an axial hydrocyclone for water separation from oil and investigated the effects of structure parameters on oil-oil separation using CFD methods. Narrowing the blade height and increasing the blade deflection angle effectively increased the rotation speed in the hydrocyclone. Therefore, increasing the blade deflection angle and decreasing the blade height can significantly increase the oil-oil separation efficiency. The small tapered angle keeps the oil droplets in the separation space for a long time, so the separation efficiency increases as the tapered angle decreases. Relatively, the reduction section of the overflow pipe had less effect on water-oil separation. However, there was a strong interaction between the reduction section and the separation efficiency. At the same time, Huang et al. [19] designed and tested the development of a high-performance dynamic hydrocyclone for water and oil separation. Dynamic hydrocyclone is a high-efficiency separator, but the oil core dispersion phenomenon was observed when the splitting ratio was small. The separated oil was mixed with water again and the separation failed. To overcome these shortcomings and improve performance, a new dynamic hydrocyclone reverse flow is derived from the conventional hydrocyclones. The results showed that in this modified dynamic hydrocyclone, air bubbles, and oil droplets were evaporated quickly from the oil outlet and the effect of interference was reduced. Therefore, the dispersion of the oil core was prevented and the separation performance was improved.

Liu et al. [20] presented research in 2019 on the innovative design and study of magnetic hydrocyclones for water and oil separation and believed that the traditional water-oil separation hydrocyclone has mainly fast separation due to the different centrifugal forces between oil and water. However, with the gradual expansion of oilfield polymers, inundation of alkaline surfactant polymer, and other oil transfer technologies, the viscosity of the fluid produced increases, and emulsification is severe, so the separation efficiency is greatly affected. Therefore, it is envisaged to add another field based on the centrifugal force field to separate the oil-water in a stronger connection field. Subsequently, the concept of a magnetic field enters the hydrocyclone. High-efficiency separation of a hydrocyclone can be achieved by bonding a centrifugal force field and a magnetic field, and they have designed a kind of magnetic hydrocyclone. In 2020, Kou and Chen [21] studied numerical fluid-fluid flow inside the hydrocyclone cylinders with guide vanes using CFD. The biphasic rotation was combined with the RSM and the mixed numerical simulation model and the results were well consistent with the experimental data. After that, more studies on the effects of the velocity field, pressure field, and separation performance under different conical angles have been studied, which shows that the intensity of

rotation and residence time has an important effect on the performance of the hydrocyclone. At the same time, Tian et al. [22] studied the decomposition of turbulent droplets by a modified concentric two-cylinder rotating device. First, according to the classical Hinze-Kolmogorov theory, the problem of droplet decomposition in a modified device was simplified. The circular flow field in the modified device was a local isotropic perturbation. Then, the high-precision turbulent RSM was used to simulate a concentric cylindrical rotating device. Their main conclusions were that the droplet size distribution corresponded to the normal input distribution when the input oil concentration was low, the integration of oil droplets was ignorable, and a new nonviscous dimensionless value was proposed.

In 2021, Wojtowicz et al. [23] analyzed the numerical and experimental analysis of the flow pattern, pressure drop, and separation efficiency in a cyclone with a square inlet and different dimensions of the rotational flow. The use of constant temperature flowmetry was confirmed. Similarly, the pressure distribution, pressure drop, and collection efficiency for cyclones were determined numerically and by measurement. In high-speed rotational flow, the rotational flow geometry affects their performance. It affects both the pressure drop and the separation efficiency for the flow model. These numerical simulations of the flow obtained the position, scale, range, and intensity of the external and internal rotational flows inside the cyclones. Increasing the length of the vortex and decreasing its diameter increased the outlet gas flow rate. Razmi et al. [24] used CFD simulation to improve the separation of hydrocyclones to decrease the biodiesel impurities. In this work, they prepared a hydrocyclone with a diameter of 10 mm. Experimental results showed a maximum impurity separation of 82.2%. Operating conditions including inlet mixture temperature, pressure drop across the hydrocyclone, and percentage of inlet impurities were optimized using the Taguchi method. Then, the hydrocyclone was modeled using CFD and the Eulerian-Eulerian computational model, and its results were confirmed using the experimental data. Zang et al. [25] increased the water flow from 3 to 7 m^3/hr and the oil fraction from 1 to 10% in an axial separator with static rotation for the oil-water mixture. The separation performance and pressure drop on the inlet flow rate and different oil fractions were studied. They found that the separation chamber using a conical tube created a greater tangential velocity than a tube with an equal diameter. Inlet flow and oil fraction were two serious operational parameters that affect the separator performance. In addition, the splitting ratio increased first and then decreased with increasing the inlet oil fraction, mainly due to a change in central pressure in the separation chamber.

Dos Anjos et al. [26] evaluated turbulent models for simulating single-phase liquid-liquid hydrocyclones. Because turbulent RSM, which is computationally expensive and difficult to converge, is more recommended in this form of computation. They selected a hydrocyclone whose experimental tangential and axial fluid flow velocity profiles were available. They resulted that the shear flow field inside the hydrocyclone may be predominant, and normal Reynolds stresses do not play an important role in predicting tangential velocities. Raeesi et al. [27] presented a three-dimensional simulation to evaluate the performance of a hydrocyclone. Due to the high-velocity rotating fluid flow, the RSM was used to model this turbulent flow. The mixed model was used to simulate multiphase flow within this hydrocyclone. The separation efficiency of the hydrocyclone was confirmed using the results of experimental data. The effect of hydrocyclone geometry and operating parameters were investigated. Finally, they provide an optimal design for high separation. They resulted that increasing the diameter of the reducing (conical) section increases the separation efficiency and the cyclone pressure drop ratio. Increasing the diameter of the conical section (cylinder) increases the separation efficiency and also the cyclone pressure drop ratio. It was also obtained that, in addition to the densities of the fluids that cause their separation based on their different flow velocities, directions, and entered centrifugal force. Consequently, other special factors, such as the wall's hydrophobic or oleophobic properties, may affect the oil-water separation efficiency of these hydrocyclones.

In the present study, the goal is to use a hydrocyclone in the oil industry to separate the liquid-liquid phases from each other. In this research, we seek to be able to separate the two fluid phases by using hydrocyclone simulation. Attending to the obtained result in our previous relevant study [27], the fluid flow inside such hydrocyclones is turbulent and the RSM and the mixture multiphase model are suitable for numerical simulation of these hydrocyclones. In this simulation, the RSM and the mixture multiphase model are used for coupling the velocity and pressure equations using the SIMPLE algorithm. The simulated geometry is taken from an experimental setup.

2. Methodology

2.1. Principles. When two liquids are mixed, they do not always become homogeneous as a solution, like water in oil. Such solutions have a common structure, such as droplets of a phase dispersed in another continuous phase, such as water in oil (W/O) or oil dispersion in water (O/W); see Figure 1. Dispersions are unstable and settle in a state of stagnation. The deposition and smoothing of the dispersions depend on the diameter of the droplets [7]. Most crude oils contain sodium and magnesium chloride, some sulfate, silica, and iron oxides. The formation of salt deposits in such a way that the phase change of water to steam occurs and the formation of hydrochloric acid causes corrosion. Hydrochloric acid is formed by the decomposition of calcium chloride and magnesium chloride at high temperatures, see equations (1) and (2). Chlorides and sulfates are soluble in small droplets of suspended water in crude oil [28]. Some of the industrial problems caused by the presence of salt solution in crude oil include corrosion in pipelines and equipment, perforation inside distillation towers, occupation of a part of tanks and fluid transmission lines, and formation of sediment and clogging of equipment.

$$CaCl_2 + 2H_2O \longrightarrow Ca(OH)_2 + 2HCl, \quad (1)$$

$$MgCl_2 + 2H_2O \longrightarrow Mg(OH)_2 + 2HCl. \quad (2)$$

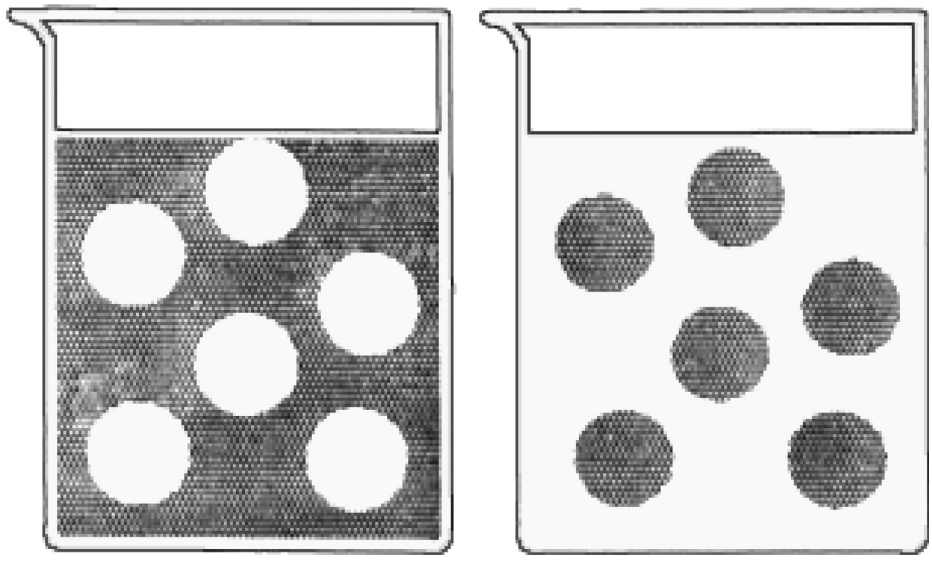

Figure 1: Dispersion of water droplets in oil and oil in water [7].

When the brine is in the form of coarse droplets, it is called dispersion, which can be separated by settling in the oil tanks. But, an emulsion may have a droplet size of about 1 micron. The separation of the phases of this emulsion is difficult because the dispersed clay particles act as a natural colloidal protector. Therefore, removing the emulsion is a basic condition for removing the brine to achieve the permissible level of 0.05% by weight. For this purpose, the chemical demulsifier, which is one of the active substances on the common surface, is used. These substances are added to crude oil in very small quantities, causing small particles to accumulate and coalesce, resulting in easy separation. Large oxygenated, sulfuric, and nitrogenous molecules in oil can also act as effective demulsifiers. Centrifugal force can also be used to increase the separation speed. Surface-active agents include fatty acid soaps, naphthenic acid, sulfonates, and even sulfonic acids. The effect of these agents can be increased by changing the pH value and increasing the temperature. The amount of required agent is about 100 to 200 grams per ton of crude oil. Here the uniform and complete distribution of the demolition solution in oil is important [29]. In recent years, the removal of salt and water from crude oil using electrical methods has become very important. Despite the different methods, their operation is based on the same principles. Also, if the salt is present in the form of fine suspended crystals in crude oil, adding enough water in the amount of 2 to 10% by volume to the oil provides the solution of microcrystalline salts at 90 to 150°C, depending on the density of crude oil [30]. Water and oil are then separated in a separate tank. This separation is either due to adding brittle emulsion chemicals or by creating a high potential electric field to accelerate the adhesion of the water droplets. In this case, alternating or direct current can be used. The required potential is between 16000 and 25000 volts [31].

Recently, hydrocyclone has been developed as a new type of water-oil separation device. It has many advantages, such as less volume, more efficiency, simpler structure, shorter residence time, high centrifugal forces (100 to 1000 times more than the gravitational acceleration), and extra. It has been shown that small changes in geometric parameters can greatly affect the separation efficiency, although the structure of the hydrocyclone is relatively simple. A hydrocyclone with a standard structure designed by experts can achieve good results for the separation of liquid water from a water-oil mixture [32]. The hydrocyclone has the characteristics of simple structure, low volume, lightweight, no moving parts, and short processing time. Therefore, it has been widely used in recent years. There is an urgent need for efficient and comprehensive water and oil separators in limited oil rigs [33, 34]. Due to the different densities of oil and water, the centrifugal force received in the hydrocyclone is different. The oil phase is less centrifugal by the centrifugal force and accumulates in the central region of the separator, while the water phase is strongly influenced by the centrifugal force and is distributed on the wall between the separators and finally achieves the separation of the mixture. Due to the small difference in density, oil and water are difficult to separate and are much harder to use in liquid-liquid cyclones than in liquid-solid cyclones.

2.2. Governing Equations. In this research, due to the high volume fraction of the discrete phase at the input, the Mixture model was used to solve the governing equations. The Mixture multiphase model is designed for two or more phases (fluid or particle). According to the Huang study [35], considering more than 10% of the volumetric fraction of desecrated phase of the water-oil mixture in the hydrocyclone, we used the Eulerian-Eulerian flow method in solving this simulation. Similar to the Eulerian multiphase model, the phases are considered intertwined chains. In the Mixture model, the momentum equation of the dissolved mixture and the relative velocities are determined to describe the dispersed phase behavior. The Mixture multiphase model, like the VOF multiphase model, uses a single-fluid

approach, but, in the Mixture model, the phases can be mixed. In the Mixture model, phases can move at different speeds using the concept of sliding velocity. In the Mixture multiphase model, the momentum, continuity, and energy equations for the mixed-phase and the volume fraction equation for the second phase are solved, such as algebraic equations for obtaining relative velocities. In this model, droplet relaxation time (*drt*) is calculated as follows:

$$\text{drt} = \frac{\left(\rho_m - \rho_p\right)d_p^2}{18\mu_f}. \tag{3}$$

Attending to the fluid densities and concentration of oil-water in the inlet mixture and also low values of the droplet sizes, in this study, the value of this parameter is about 1.2×10^{-4} sec which is smaller than 0.001 sec, which is the maximum acceptable value for *drt* in the mixture model [36]. In this mode, the continuity equation is presented below [36]:

$$\frac{\partial}{\partial t}\left(\rho_m\right) + \nabla\cdot\left(\rho_m\overrightarrow{v_m}\right) = 0, \tag{4}$$

where t is the time, ρ_m is the density of the mixture, and $\overrightarrow{v_m}$ is the average velocity vector of a mass calculated from the following equations:

$$\overrightarrow{v_m} = \frac{\sum_{k=1}^{n}\alpha_k\rho_k v_k}{\rho_m}, \tag{5}$$

$$\rho_m = \sum_{k=1}^{n}\alpha_k\rho_k, \tag{6}$$

where ρ_k is the density and α_k is the volume fraction of phase k. The volume fraction of this phase is obtained from the following equation:

$$\frac{\partial}{\partial t}\left(\alpha_k\rho_k\right) + \nabla\cdot\left(\alpha_k\rho_k\overrightarrow{v_m}\right) = -\nabla\cdot\left(\alpha_k\rho_k\overrightarrow{v_{dr,k}}\right), \tag{7}$$

where $\overrightarrow{v_{dr,k}} = \overrightarrow{v_k} - \overrightarrow{v_m}$ is the drift velocity vector of the phase k that can be calculated as follows:

$$\overrightarrow{v_{dr,p}} = \overrightarrow{v_{pq}} - \sum_{k=1}^{n}\frac{\alpha_k\rho_k}{\rho_m}\overrightarrow{v_{qk}}, \tag{8}$$

where $\overrightarrow{v_{pq}} = \overrightarrow{v_p} - \overrightarrow{v_q}$ is the relative velocity of p and q phases that is calculated as below:

$$\overrightarrow{v_{pq}} = \frac{\left(\rho_p - \rho_m\right)d_p^2}{18\mu_q f_{\text{drag}}}\overrightarrow{a}, \tag{9}$$

where d_p is the droplet diameter, f_{drag} is the drag function, and $\overrightarrow{a}$ is the acceleration vector of the droplet, which have been calculated using the following equations:

$$f_{\text{drag}} = \begin{cases} 1 + 0.15\text{Re}^{0.687}, & \text{Re} \le 1000, \\ 0.0183\text{Re}, & \text{Re} > 1000, \end{cases} \tag{10}$$

$$\overrightarrow{a} = \overrightarrow{g} - \left(\overrightarrow{v_m}\cdot\overrightarrow{\nabla}\right)\overrightarrow{v_m} - \frac{\partial\overrightarrow{v_m}}{\partial t}, \tag{11}$$

where $\overrightarrow{g}$ is the gravitational acceleration vector. The momentum equation for the mixture can be obtained by summing the momentum equations of the individual phases for all phases. It can be expressed as follows [36]:

$$\frac{\partial}{\partial t}\left(\rho_m\overrightarrow{v_m}\right) + \nabla\cdot\left(\rho_m\overrightarrow{v_m}\overrightarrow{v_m}\right) = -\nabla P + \nabla\cdot\left[\mu_m\left(\nabla\overrightarrow{v_m} + \nabla\overrightarrow{v_m^T}\right)\right] + \rho_m\overrightarrow{g} + \overrightarrow{F} + \nabla\cdot\left(\sum_{k=1}^{n}\alpha_k\rho_k\overrightarrow{v_{dr,k}}\overrightarrow{v_{dr,k}}\right). \tag{12}$$

Here n is the number of phases, P is the pressure, $\overrightarrow{F}$ is the vector of external forces, and μ_m is the viscosity of the mixture.

$$\mu_m = \sum_{k=1}^{n}\alpha_k\mu_k. \tag{13}$$

To model turbulent fluid flows, there are many turbulent flow models, ranging from k-ε models to more complex Reynolds Stress Models. The choice of a suitable model for highly rotational flow within a hydrocyclone has been studied by many researchers [37, 38]. The turbulent Reynolds Stress Model is able to accurately predict rotational flow behavior at high velocities, and its results are near to the actual results. For this model, it is necessary to solve the transfer equations for each of the Reynolds stresses, which allows the turbulent flow pattern, axial velocity, tangential velocity, shear diameter, and pressure drop in rotational flows to be properly simulated. Because this model calculates the effects of flow line curvature, rotation, and rapid changes in strain rate in a more difficult way than other turbulence models, it has a higher potential for accurately predicting complex flows [39, 40]. In this model, the transfer equation is written as follows [41]:

$$\frac{\partial}{\partial t}\left(\rho\overline{u_i'u_j'}\right) + \frac{\partial}{\partial x_k}\left(\rho u_k\overline{u_i'u_j'}\right) = D_{ij} + P_{ij} - \Phi_{ij} + \varepsilon_{ij}. \tag{14}$$

The two sentences on the left side of this equation represent the local derivative of stress with respect to the time and the sentence related to convective transfer, respectively. If the fluid flow is stable, the stress derivative with respect to the time will be zero. The four terms on the right side of this equation have been presented in equations (15)–(18).

$$D_{ij} = -\frac{\partial}{\partial x_k}\left[\overline{u_i'u_j'u_k'} + P'\left(\delta_{kj}u_j' + \delta_{ik}u_j'\right)\right] + \frac{\partial}{\partial x_k}\left[\mu_m\frac{\partial}{\partial x_k}\left(\overline{u_i'u_j'}\right)\right]. \tag{15}$$

This equation is related to the stress penetration, where P' and u' are the fluctuations of the pressure and velocity and δ is the Kronecker delta. The first term of this equation represents the penetration of the turbulent and the second term represents the molecular penetration.

$$P_{ij} = -\rho_m\left(\overline{u_i'u_k'}\frac{\partial u_j}{\partial x_k} + \overline{u_i'u_k'}\frac{\partial u_i}{\partial x_k}\right). \tag{16}$$

This equation is related to the Reynolds stress generation.

$$\Phi_{ij} = \overline{P'\left(\frac{\partial u_i'}{\partial x_j} + \frac{\partial u_j'}{\partial x_i}\right)}. \quad (17)$$

This equation is related to stress pressure.

$$\varepsilon_{ij} = -2\mu_m \overline{\frac{\partial u_i'}{\partial x_j}\frac{\partial u_j'}{\partial x_i}}. \quad (18)$$

This equation is about the loss of disturbed kinetic energy.

2.3. Numerical Method. In the CFD method, by converting the governing fluid differential equations to algebraic equations, it is possible to solve these equations numerically. By dividing the desired area of analysis into smaller elements and applying boundary conditions to the boundary nodes, by considering approximations, a system of linear equations is obtained, which with solving the algebraic equations obtains the field of velocity, pressure, and temperature in the desired area. To model a system, we must first generate the geometry we want to use. The generated geometry must then have meshed. Meshing has an important role in solving the problem. According to Figure 2 and Table 1, the geometry of the hydrocyclone is defined.

To solve a CFD problem, a fundamental step is taken in the preprocessing, processing, and postprocessing sectors. Mesh generation is in the preprocessing part. In this research, according to Figure 2, after producing a suitable and accurate geometry of the problem, the existing geometry was divided into a series of grids or discrete elements. The choice of an approach in mesh generation depends on three factors: accuracy, efficiency, and ease of generation. Accuracy means the desired quality of the mesh, which is defined by various standards and criteria. The most famous of them is the unevenness or skewness of the mesh, the criterion of orthogonal quality and aspect ratio, in which all three parameters are in a good area. Efficiency refers to the efficiency of the desired number of cells. Due to the knowledge of flow in this problem, in the sections where the changes are more severe, the network has become smaller. Ease of mesh generation is the basic parameter in this section. In general, the production of disorganized mesh is faster and in contrast to the generation of meshes with an organization or a combination is time-consuming. In this case, we have used a hybrid hexagonal mesh. The advantage of the hexagonal mesh is that while our cell number is low, this network is generated in the shortest time, and the accuracy of calculations in this type of mesh structure is high.

The boundary conditions for this geometry are in three areas: input, output, and wall. In the inlet area where the fluid is injected tangentially into the hydrocyclone, the velocity of the fluid entering this area is known and the flow rate is determined by the hydraulic diameter and the inlet velocity, and the intensity of the turbulence. The volume

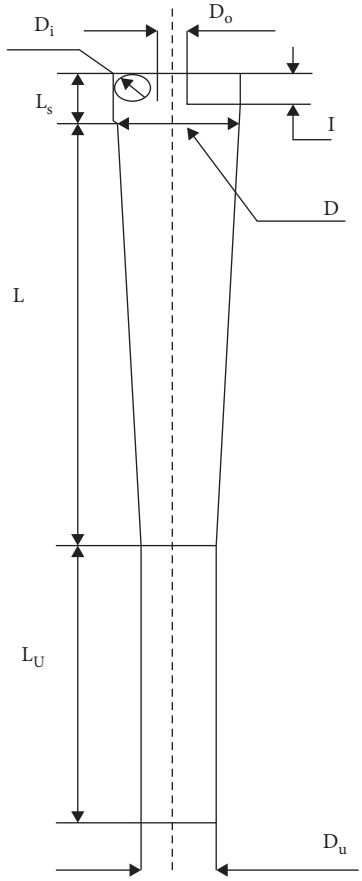

Figure 2: Hydrocyclon geometry.

fraction of the discrete phase is determined based on experimental data. In hydrocyclone geometry, there are two areas for the fluid exit, one at the top of the hydrocyclone and the other at the bottom. Because in the hydrocyclone, a rotational fluid flow is generated in the direction of the radius and causes changes in pressure, the pressure is important. The no-slip condition has been defined for the wall boundary condition. In this simulation, a combination of two phases of water and oil solution (with the presented properties in Table 2) is injected into the inlet section of the mentioned hydrocyclone.

To find the velocity distribution, the Navier-Stokes equations are solved together with the RSM equations. The QUICK scheme is used to obtain the momentum equations and the quadratic discretization method is used to obtain the kinetic energy of the turbulence and the turbulence rate. Due to the fact that a rotating fluid flow is generated inside the hydrocyclone, the PRESTO method has been used for pressure discretization and the SIMPLE method has been used for the relationship between pressure and velocity. The acceptable accuracy for the calculated values in this numerical solution was considered equal to 10^{-6} (according to Figure 3).

3. Results and Discussion

3.1. Mesh Independency. One of the important parameters in the simulation process is the independence of the obtained

Table 1: The size of different sections of the investigated hydrocyclone [42].

D (mm)	I (mm)	Do (mm)	Di (mm)	Ls (mm)	L (mm)	Lu (mm)	Du (mm)
35	9.8	15.15	7	10.01	380.8	299.6	10.01

Table 2: Feed properties [42].

Phase	%	Density (kg/m^3)	Viscosity (kg/m/s)
Water	75	998.2	0.001
Oil	25	882	0.005

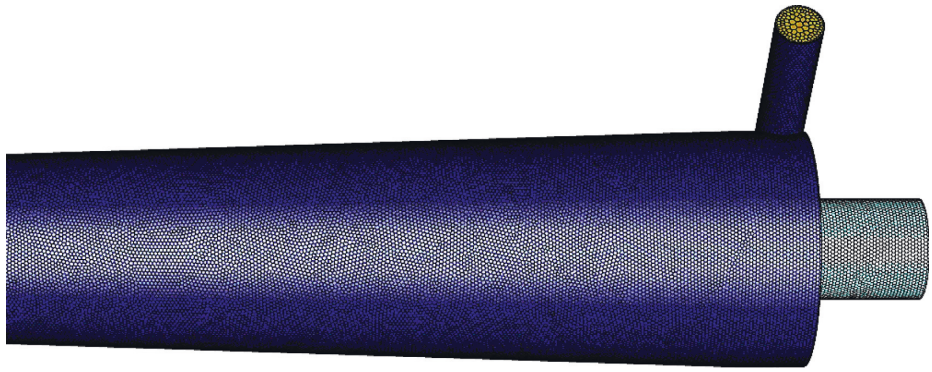

Figure 3: A view of the hydrocyclone mesh.

results from the number of mesh elements. The results obtained should not depend on the number of cells in the computing grid. In this research, different numbers of grids (681546, 992280, and 1045811) have been analyzed. Tangential velocity parameters at different radiuses and separation efficiencies have been obtained in these meshes, and the obtained data have been presented in Figure 4 and Table 3. The results obtained from the defined mesh with 681546 calculation nodes are far from the two other cases and the experimental data. On the other hand, attending to the high computation cost of the mesh with 1045811 calculation nodes, the defined mesh with 992280 nodes has been accepted for a suitable simulation in this hydrocyclone.

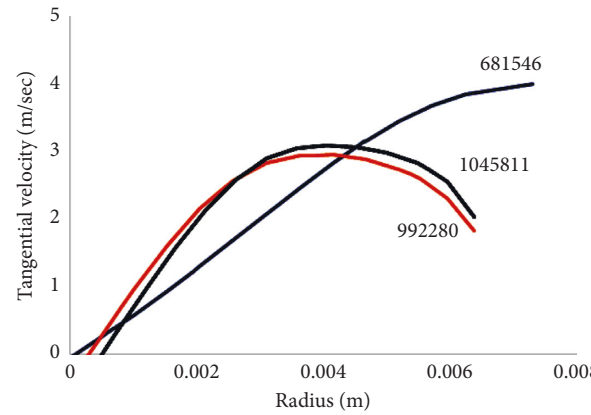

Figure 4: Calculation of tangential velocity versus radiuses if the hydrocyclone with different calculation meshes.

3.2. Validation. In order to use the simulation results, the simulation results must first be compared with the experimental data for acceptance of the predictions of the developed model. It is observed in Figure 5 that the calculated separation efficiency (Seperation Efficiency = Mass flowrate of outlet oil from top offload/Mass flowrate of inlet oil) by this simulation has less than a ten percent difference from the experimental data obtained by Prataran et al. [42]. Attending to the complexity of this problem, this range of error of the validated results is acceptable [35]. We have calculated the mass balance (for total flow and also water and oil components) for validating the model predictions. The maximum calculated value for relative error between inlet and outlet flows was equal to 2.65×10^{-7}, which is lower than our convergence condition acceptance value (*i.e.,* 10^{-6}). Therefore, the simulation results are valid and the predicted results can be used.

3.3. The Effect of the Fluid Flow Directions and the Forces on the Hydrocyclone Efficiency. In a hydrocyclone, there are many forces in which the centrifugal force and the fluid resistance (drag) account for the largest share of the separation efficiency. In this equipment, fluid directions are in two opposite directions, so that the centrifuge force directs the fluid toward the wall, but the drag force directs the fluid toward the core of the hydrocyclone. Therefore, the lighter fluid has a larger volume of drag force, and the heavier fluid has a larger volume of centrifugal force.

Figure 6 shows the direction of flow inside the hydrocyclone. There are two types of rotational flows inside the hydrocyclone. The fluid enters the cylindrical part of the

Table 3: Hydrocyclone separation efficiencies in different calculation meshes.

Run	Mesh type	Size	Separation efficiency (%)
1	Large	681546	59
2	Medium	992280	71
3	Small	1045811	73

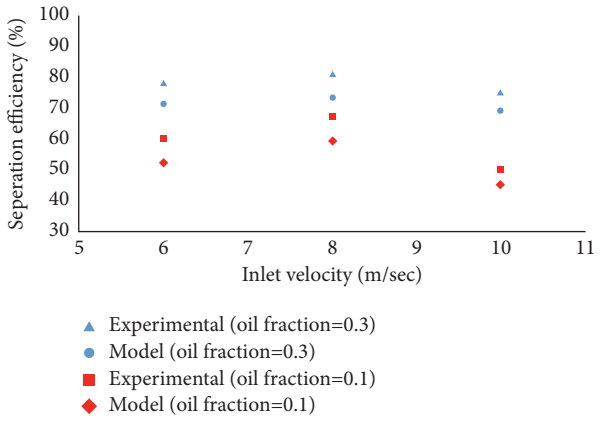

Figure 5: Comparison of simulation results with experimental data [42].

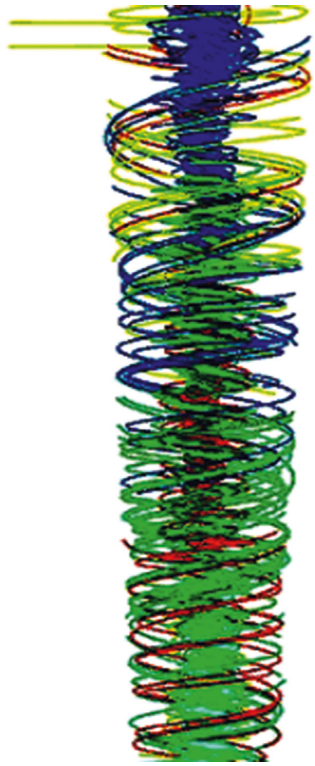

Figure 6: Streamlines of the continuous phase (water).

hydrocyclone tangentially, and then it is divided into two internal and external rotational flows. A large part of the fluid, which includes the continuous phase of water and also has a higher density than the discrete phase, moves toward the wall of the hydrocyclone and exits the bottom, and thus the discrete phase fluid, which has a lower density than the continuous phase, enter the internal rotation, moves upwards and exits from the upper part of the hydrocyclone (overflow).

3.4. Investigation of the Fluid Flow Velocity and Pressure inside the Hydrocyclone. Figure 7 shows the static pressure inside the hydrocyclone. Due to the rotational current created by the tangential inlet flow, there are variations in the pressure, in the radial and axial directions. According to this figure, after entering the hydrocyclone, the fluid flow is divided into two different flows with different pressures. In the yellow area, the high pressure is formed by the heavier and denser fluid, which moves toward the walls by the centrifugal force because the pressure builds up near the wall. The dark blue area has negative pressure, and the lighter fluid, which has a lower density, moves toward the lower pressure hydrocyclone core by a rotational flow and has been separated from the heavier phase, consequently.

As shown in Figure 8, the input fluid flow velocity plays an important role in the separation efficiency process. It should be noted that we tried to study a simple structure of hydrocyclones for this separation, which has a minimum operating cost in comparison with hydrocyclones with rotating impellers, magnetic forces, or extra. Therefore, no external force has been considered for the simulated hydrocyclone. Since no external dynamic force is used in the hydrocyclone, the flow velocity fluctuation is the only parameter that affects the separation efficiency. To make the best use of the hydrocyclone and get more efficiency, we can increase the input fluid flow velocity. However, according to the obtained results, after passing a certain inlet velocity value, the efficiency has decreased. It should be noted that the relative velocities among the fluid flow layers within the circular flows inside these hydrocyclones have a major role in the generation of eddies in the high intralayer shear stress zones. Increasing the inlet fluid flow velocity (more than a certain value), increases the velocity difference among the fluid flow layers, increases the shear stresses among these layers, increases the eddies generations zones, and increases the mixing effects by these eddies, consequently.

3.5. Separation of Discrete Phase (Water) from Continuous Phase (Oil). In this stage of the study, it is considered that the inlet fluid flow consists of 25% oil and 75% water. Our goal in this section is to separate the phases with the best efficiency. Based on this research with a droplet size from 20 to 200 microns, it is founded that the lower density phase moves toward the hydrocyclone core, and the denser phase moves toward the wall. According to Figure 9, the oil phase separation has been increased by increasing its droplet size from 20 to 100 microns, and from 100 to 200 microns, the separation performance has been almost constant, which means that approximately 99.5% of the oil has been separated from the water. Therefore, it is better to consider a series of processes to increase the diameter of the oil droplets before entering the hydrocyclone. The modeled sizes of the droplet in this simulation are in the normal range of the investigated droplets in different studies [12, 13, 22]. In industrial applications, this size can be utilized, bypassing the discrete phase from specially designed sieves.

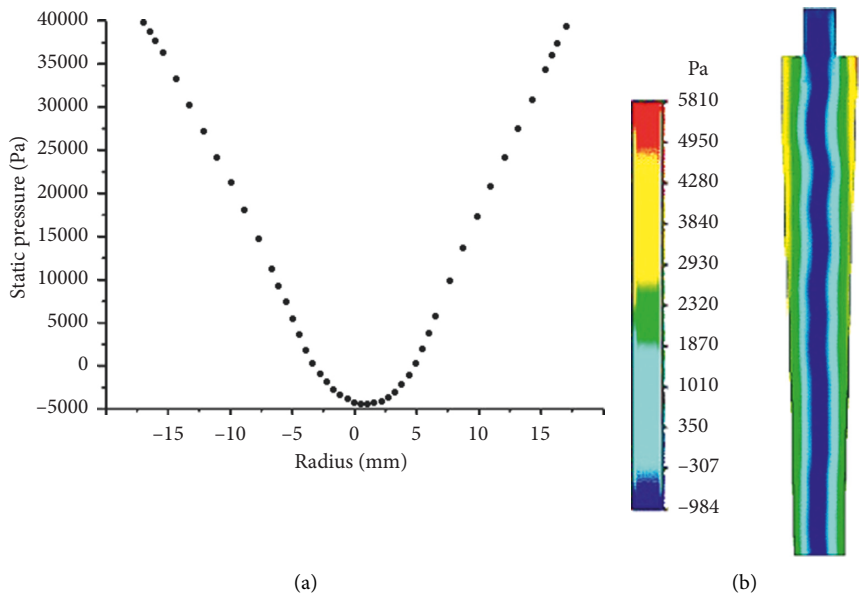

Figure 7: (a) Static pressure diagram and (b) contour, within the hydrocyclone.

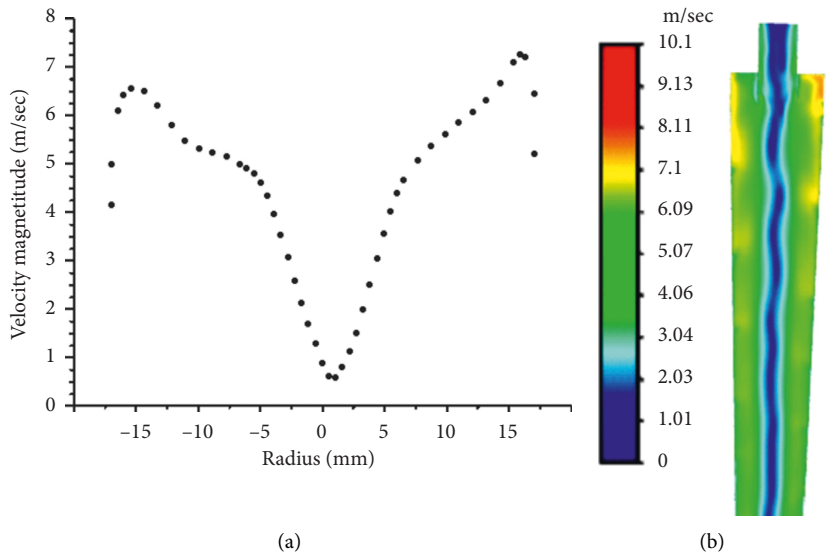

Figure 8: (a) Diagram and (b) contour of velocity magnitude within the hydrocyclone.

3.6. Separation of Discrete Phase (Water) from Continuous Phase (Oil). In this part of the study, it is considered that the inlet fluid flow to the hydrocyclone consists of 90% oil and 10% water. According to Table 4, in three different inlet velocities with a certain diameter of water droplets (i.e., 75 microns), it is obtained that at 8 m/sec, inlet velocity has the highest separation efficiency.

At inlet velocity equal to 6 m/sec, it is observed that the lowest separation efficiency has been achieved because fewer droplets of water move down the wall of the hydrocyclone, and the forces have no important effects at this velocity. Therefore, the rest of the water with the oil comes out from the overflow and keeps the separation efficiency at the 40% level. At an inlet velocity equal to 8 m/sec, the maximum efficiency has been achieved so that using this inlet velocity, we can separate these two phases in the best possible way. In this case, the internal and external flows work properly, so that the effect of the forces is noticeable, according to Figure 10. Therefore, more water comes out from the bottom, resulting in 48% separation efficiency. At 10 m/sec inlet velocity, the separation efficiency has been decreased because the effect of the forces on the phases has been decreased, so the separation efficiency of these two phases has been reduced to 43%.

In this section, the results of simulations with water droplets with sizes equal to 150, 75, and 200 microns have been presented. As can be seen in Table 5, the separation efficiency has been increased up to approximately 70% as the droplet diameter was increased. According to the centrifugal force equation, the higher the mass of the droplet, the larger

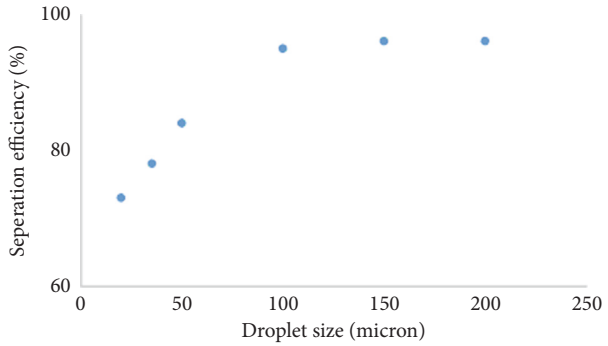

Figure 9: Effect of droplet size on the separation efficiency.

Table 4: Efficiency of water separation in the bottom.

Run	Inlet fluid flow velocity (m/sec)	Water separation efficiency (%)
1	6	40
2	8	48
3	10	42

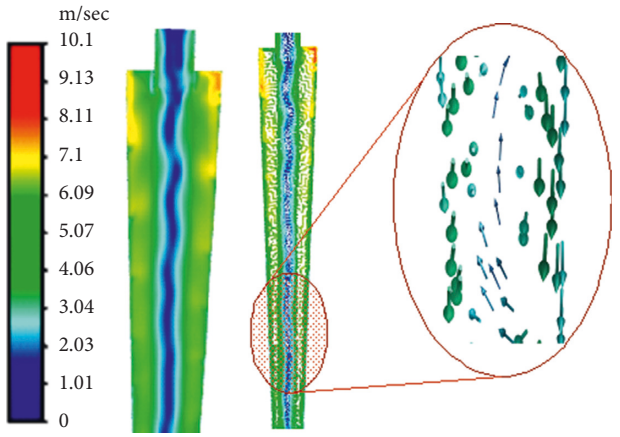

Figure 10: The fluid flows vectors inside the hydrocyclone.

Table 5: The effect of water droplet diameter on the separation efficiency.

Run	Water droplet size (micron)	Water separation efficiency at the bottom (%)
1	75	48
2	150	60
3	200	69

the centrifugal force. It causes water droplets to move toward the wall of the hydrocyclone. Water droplets also move downwards under the influence of gravity.

4. Conclusions

In this research, a homemade code has been developed to simulate the separation of two fluids, water, and oil, using a hydrocyclone device. The three-dimensional geometry of the hydrocyclone has first meshed. Then, to solve the problem, the Reynolds stress turbulence model and mixed multiphase model were used, and then the governing equations were solved, numerically. The results obtained from the simulation model were compared with the existing experimental data. The difference between the simulation results and the experimental data was less than 10%. The Reynolds stress perturbation model predicted the flow pattern stress in the hydrocyclone, which was observed in two types of rotational flow. The free rotational flow moves to the bottom and the forced rotational flow moves to the overflow. The following results have been obtained in this study:

(i) In the case where 25% of the inlet fluid flow to the hydrocyclone consists of oil, as the droplet diameter increases, the separation efficiency increases, and when the droplet diameter exceeds 100 microns, the separation efficiency increases to 99.5%, because the affected drag and buoyancy forces to the oil droplets increase and therefore the discrete phase moves toward the hydrocyclone core.

(ii) Separation efficiency is directly related to inlet velocity up to 8 m/sec. This means that as the inlet velocity increases, the separation efficiency also increases, and from a certain velocity (i.e., 8 m/sec), the separation efficiency is inversely related to this parameter. More than this value, the higher the inlet velocity, the lower the separation efficiency. This is because the higher the inlet velocity, the greater the centrifugal force than the drag force, so it causes some of the discrete phases to move toward the wall, which reduces the separation efficiency.

(iii) In the case that the fluid entering the hydrocyclone is 10% water and the rest is oil, more of the water comes out from the bottom. It is concluded that the larger the diameter of the water droplets, the larger the percentage of water exiting from the bottom. In this simulation, the diameter of the water droplets was increased to 150 microns. In this case, 60% of the water entering the hydrocyclone is discharged from the bottom.

Nomenclature

a: Acceleration of droplet $(m \cdot s^{-2})$
d_p: Droplet diameter (m)
D_{ij}: Stress penetration
f_{drag}: Drag function
$\vec{F}$: Vector of external forces
g: Acceleration caused by an external physical force $(m \cdot s^{-2})$
k: The turbulent kinetic energy $(J \cdot kg^{-1})$
n: number of phase
$\overline{P}$: Average pressure (Pa)
P_{ij}: Reynolds stress generation
P_k: The rate of production of turbulence kinetic energy [32]: $P_k = -\overline{u_i' u_j'} \partial u_i / \partial x_j$
Re_t: Reynolds number of turbulence flow [9]: $\text{Re}_t = k^2 / \upsilon\varepsilon$

$\overline{u_i}$, $\overline{u_j}$: Components of the average velocity vector $(m \cdot s^{-1})$: $\overline{u}$, $\overline{v}$
u_i', u_j': Components of the turbulent velocity vector $(m \cdot s^{-1})$: u', v'
$\overline{v'^2}$ / $\overline{u_i' u_j'}$: Reynolds stress components $(m^2.\, s^{-2})$: $\overline{u'v'}$, $\overline{u'^2}$
v: average velocity
t: time (s)

Greek Letters

α: Volume fraction
δ_{ij}: Kronecker delta $\delta_{ij} = \begin{cases} 1 & i = j \\ 0 & i \neq j \end{cases}$
ε_{ij}: Turbulent kinetic energy dissipation rate $(J \cdot kg^{-1})$
μ: The viscosity of fluid $(Pa \cdot s)$
μ_t: Turbulent viscosity of the flow based on the k-ε model $(Pa \cdot s)$ [2]: $\mu_t = C_\mu f_\mu \rho k^2/\varepsilon$
υ: Kinematic viscosity of the fluid $(m^2 \cdot s)$
ρ: Density of the fluid $(kg \cdot m^{(-3)})$
Φ_{ij}: Stress pressure
$\nabla \cdot u$: Divergence of u vector

Suscripts

k, p, q: related to the phases
m: mixture.

Data Availability

No data were used in this study.

Conflicts of Interest

The authors declare that they have no conflicts of interest.

References

[1] H. K. Abdel-Ail, A. Mohamed, and M. A. Fahim, *Petroleum and Gas Field Processing*, CRC Press, Boca Raton, FL, USA, 2015.

[2] J. H. Gary, G. E. Handwerk, and M. J. Kaiser, *Petroleum Refining-Technology and Economics*, CRC Press, Boca Raton, FL, USA, 2007.

[3] G. Liu, X. Xu, and J. Gao, "Study on the compatibility of high-paraffin crude oil with electric desalting demulsifiers," *Energy & Fuels*, vol. 17, no. 3, p. 630, 2003.

[4] Y. J. Wang and J. T. Cui, "The experiment of dehydration from crude oil by centrifuge," *Chinese Oil-Gasfield Surface Engineering*, vol. 16, no. 3, pp. 19–22, 1997.

[5] K. T. Hsieh and R. K. Rajamani, "Mathematical model of the hydrocyclone based on physics of fluid flow," *AIChE Journal*, vol. 37, no. 5, pp. 735–746, 1991.

[6] C. Gomez, J. Caldentey, S. Wang, L. Gomez, R. Mohan, and O. Shoham, "Oil-water separation in liquid-liquid hydrocyclones (LLHC)-experiment and modeling," in *Proceedings of the SPE Annual Technical Conference and Exhibition*, New Orleans, LA, USA, September 2001.

[7] M. Jiang, L. Zhao, and Z. Wang, "Effects of geometric and operating parameters on pressure drop and oil-water separation performance for hydrocyclones," in *Proceedings of the Twelfth International Offshore and Polar Engineering Conference*, Kitakyushu, Japan, May 2002.

[8] M. A. Reyes, J. E. Pacheco, N J. C. Mari´, L. R. Rojas, and N J. Rincon´, "Numerical simulation and experiments of the multiphase flow in a liquid-liquid cylindrical cyclone separator," *Fluids Engineering Division Summer Meeting*, vol. 1, pp. 667–673, 2006.

[9] K. U. Bhaskar, Y. R. Murthy, M. R. Raju, S. Tiwari, J. K. Srivastava, and N. Ramakrishnan, "CFD simulation and experimental validation studies on hydrocyclone," *Minerals Engineering*, vol. 20, no. 1, pp. 60–71, 2007.

[10] T. Husker, O. Rameau, T. Dragster, and T. Bilstad, "Performance of a Deoilin hydrocyclone during variable flow rates," *Minerals Engineering*, vol. 20, no. 4, pp. 368–379, 2007.

[11] Z. S. Bai and H. L. Wang, "Crude oil desalting using hydrocyclones," *Chemical Engineering Research and Design*, vol. 85, no. 12, pp. 1586–1590, 2007.

[12] S. Y. Shi, Y. X. Wu, J. Zhang, J. Guo, and S. J. Wang, "A study on separation performance of a vortex finder in a liquid-liquid cylindrical cyclone," *Journal of Hydrodynamics*, vol. 22, no. S1, pp. 380–386, 2010.

[13] F. L. Zhang, S. S. Deng, and W. X. Hua, "Numerical simulation for flow field in hydrocyclone," *Advanced Materials Research*, vol. 335, pp. 683–687, 2011.

[14] D. Mowlam Amini S, D. Mowla, M. Golkar, F. Esmaeilzadeh, and F. Esmaeilzadeh, "Mathematical modelling of a hydrocyclone for the down-hole oil–water separation (DOWS)," *Chemical Engineering Research and Design*, vol. 90, no. 12, pp. 2186–2195, 2012.

[15] M. Narasimha, M. S. Brennan, and P. N. Holtham, "CFD modeling of hydrocyclones: prediction of particle size segregation," *Minerals Engineering*, vol. 39, pp. 173–183, 2012.

[16] S. M. Hosseini, K. Shahbazi, and M. R. Khosravi Nikou, "A CFD simulation of the parameters affecting the performance of downhole de-oiling hydrocyclone," *Iranian Journal of Oil & Gas Science and Technology*, vol. 4, no. 3, pp. 77–93, 2015.

[17] T. R. Vakamalla and N. Mangadoddy, "Numerical simulation of industrial hydrocyclones performance: role of turbulence modelling," *Separation and Purification Technology*, vol. 176, pp. 23–39, 2017.

[18] M. Liu, J. Chen, X. Cai, Y. Han, and S. Xiong, "Oil–water preseparation with a novel axial hydrocyclone," *Chinese Journal of Chemical Engineering*, vol. 26, no. 1, pp. 60–66, 2018.

[19] L. Huang, S. Deng, J. Guan, M. Chen, and W. Hua, "Development of a novel high-efficiency dynamic hydrocyclone for oil–water separation," *Chemical Engineering Research and Design*, vol. 130, pp. 266–273, 2018.

[20] L. Liu, L. Zhao, X. Yang, Y. Wang, B. Xu, and B. Liang, "Innovative design and study of an oil-water coupling separation magnetic hydrocyclone," *Separation and Purification Technology*, vol. 213, pp. 389–400, 2019.

[21] J. Kou, Y. Chen, and J. Wu, "Numerical study and optimization of liquid-liquid flow in cyclone pipe," *Chemical Engineering and Processing-Process Intensification*, vol. 147, Article ID 107725, 2020.

[22] Y. Tian, Y. Tian, G. Shi, B. Zhou, C. Zhang, and L. He, "Experimental study on oil droplet breakup under the action of turbulent field in modified concentric cylinder rotating device," *Physics of Fluids*, vol. 32, no. 8, Article ID 087105, 2020.

[23] R. Wójtowicz, P. Wolak, and A. Wójtowicz-Wróbel, "Numerical and experimental analysis of flow pattern, pressure drop and collection efficiency in a cyclone with a square inlet

and different dimensions of a vortex finder," *Energies*, vol. 14, no. 1, p. 111, 2020.

[24] F. Salmanizade, A. Ghazanfari Moghaddam, and A. Mohebbi, "Improvement hydrocyclone separation of biodiesel impurities prepared from waste cooking oil using CFD simulation," *Separation Science and Technology*, vol. 56, no. 6, pp. 1152–1167, 2021.

[25] X. Zeng, L. Zhao, W. Zhao et al., "Experimental study on a compact axial separator with conical tube for liquid-liquid separation," *Separation and Purification Technology*, vol. 257, Article ID 117904, 2021.

[26] R. P. dos Anjos, R. D. Andrade Medronho, and T. Suaiden Klein, "Assessment of turbulence models for single phase CFD computations of a liquid-liquid hydrocyclone using OpenFOAM," *Journal of Turbulence*, vol. 22, no. 2, pp. 79–113, 2021.

[27] S. Raeesi, A. Soltani Goharrizi, and B. Abolpour, "Numerical investigation of a hydro-cyclone for separating organic and aqueous phases," *Journal of the Institution of Engineers: Series C*, vol. 102, no. 4, pp. 995–1005, 2021.

[28] Y. Tanaka, "The effect of solution leakage in an ion-exchange membrane electrodialyzer on mass transport across a membrane pair," *Journal of Membrane Science*, vol. 231, no. 1-2, pp. 13–24, 2004.

[29] M. Al-Otaibi, A. Elkamel, T. Al-Sahhaf, and A. S. Ahmed, "Experimental investigation of crude oil desalting and dehydration," *Chemical Engineering Communications*, vol. 190, no. 1, pp. 65–82, 2003.

[30] V. V. Popp and V. D. Dinulescu, "Dehydration and desalting of heavy and viscous crude oil produced by in-situ combustion," *SPE Production and Facilities*, vol. 12, no. 2, pp. 95–99, 1997.

[31] R. A. Mohammed, A. I. Bailey, P. F. Luckham, and S. Taylor, "Dewatering of crude oil emulsions 3. Emulsion resolution by chemical means," *Colloids and Surfaces A: Physicochemical and Engineering Aspects*, vol. 83, no. 3, pp. 261–271, 1994.

[32] L. Vafajoo, K. Ganjian, and M. Fattahi, "Influence of key parameters on crude oil desalting: an experimental and theoretical study," *Journal of Petroleum Science and Engineering*, vol. 90-91, pp. 107–111, 2012.

[33] L. F. Martínez, A. G. Lavín, M. M. Mahamud, and J. L. Bueno, "Improvements in hydrocyclone design flow lines stabilization," *Powder Technology*, vol. 176, pp. 1–8, 2007.

[34] L. F. Martínez, A. G. Lavín, M. M. Mahamud, and J. L. Bueno, "Vortex finder optimum length in hydrocyclone separation," *Chemical Engineering and Processing: Process Intensification*, vol. 47, no. 2, pp. 192–199, 2008.

[35] FLUENT.INC Press, Part18: "Mixture model theory".

[36] S. Huang, "Numerical simulation of oil-water hydrocyclone using ReynoldsStress model for eulerian multiphase flows," *Canadian Journal of Chemical Engineering*, vol. 83, no. 5, pp. 829–834, 2008.

[37] W. Griffiths and F. Boysan, "Computational fluid dynamics (CFD) and empirical modelling of the performance of a number of cyclone samplers," *Journal of Aerosol Science*, vol. 27, no. 2, pp. 281–304, 1996.

[38] T. Chuah, J. Gimbun, and T. S. Choong, "A CFD study of the effect of cone dimensions on sampling aerocyclones performance and hydrodynamics," *Powder Technology*, vol. 162, no. 2, pp. 126–132, 2006.

[39] N. Kharoua, L. Khezzar, and Z. Nemouchi, "CFD simulation of liquid-liquid hydrocyclone: oil/water application," in *Proceedings of the ASME 2009 Fluids Engineering Division Summer Meeting*, pp. 2085–2094, Vail, CO, USA, August 2009.

[40] R. Maddahian, B. Farhanieh, S. D. Saemi, and T. Bilstad, "Numerical simulation of deoilin hydrocyclones," *World Academy of Science, Engineering and Technology*, vol. 59, pp. 2044–2049, 2011.

[41] Fluent.INC Press, Part4: "Turbulence Model ".

[42] W. Pratarn, S. Kanawut, and S. Thanit, "Experimental investigation of de-oiling hydrocyclone," *InKey Engineering Materials*, vol. 545, pp. 230–235, 2013.